Numerical investigation and modeling of residual stress field variability impacting the machining deformations of forged part

Hugo Chabeauti, Mathieu Ritou, Bruno Lavisse, Guenael Germain, Virginie Charbonnier

Available online at www.sciencedirect.com

ScienceDirect

Procedia CIRP 108 (2022) 687–692

www.elsevier.com/locate/procedia

6th CIRP Conference on Surface Integrity

Numerical investigation and modeling of residual stress field variability impacting the machining deformations of forged part

Hugo Chabeauti[a,b,c]*, Mathieu Ritou[b], Bruno Lavisse[a], Guenael Germain[a], Virginie Charbonnier[c]

[a]*LAMPA, Arts et Métiers ParisTech, Campus d'Angers, 2 bd du Ronceray, Angers 49035, France*
[b]*LS2N (Laboratory of Digital Sciences of Nantes, UMR CNRS 6004), university of Nantes, 1 Quai de Tourville, Nantes 44000, France*
[c]*Airbus Operations, rue de l'aviation, Bouguenais 44340, France*

* Corresponding author. Tel.: +33 640646156. *E-mail address:* hugo.chabeauti@ensam.eu

Abstract

Aluminum alloys are widely used for structural parts in the aerospace industry. Those parts are usually machined from rolled plates or forged blanks, and heat treatments are carried out to reach the necessary mechanical properties. Forming and heat treatments induce residual stresses that generate deformations during and after machining because material removal modifies their balance. One major issue in industry is the important variability of the residual stress field in forged blanks. A better knowledge of the residual stress field will enable the definition of better machining strategy to minimize the deformations. In order to understand and manage this variability, a sensibility analysis was performed to investigate the impact of their different potential sources. It relies on a coupling of 2D-FEM and beam model simulations. Then, this work introduces a model reduction technique (by POD and SVD) to build a model of the variability of a stress field and shows how it could be used on the production line.

Keywords: Residual stresses; Deformations; Machining; Forge

1. Introduction

Aluminum alloys are widely used in the aerospace industry for their high mechanical properties. Numerous structural parts in modern aviation are machined from 7000 series aluminum alloy for their high strength and corrosion resistance. To reach those high mechanical characteristics rolled plates or forged blanks go through heat treatments such as quenching followed by tempering. During the processing of the part, the plastic and thermal deformation gradients induce residual stresses which can be of high intensity [1]. During machining, the balance of these stresses is modified, which leads to large deformations of the part at the unclamping. Indeed, when unclamping the part, the part distorts to return to a balanced stress field. The thermo-mechanical loads due to machining can also introduce residual stresses on the part surface [2]. The affected depth is relatively shallow, less than a few hundred microns [3]. In thin parts, these stresses cannot be neglected because they can also provoke deformation of the part. However, for massive parts, these stresses induced by machining can be neglected, compared to those released by cutting [4]. For large aeronautical parts, an additional reshaping step is often necessary, so that the part would meet the required geometrical specifications before assembly, which increases the cost. To reduce the deformations, the part can be stretched or compressed plastically to homogenize the stress field [5]. Only compression is possible for curved parts. The deformation of the part after machining depends on the stresses released. It will therefore vary in relation to the stress field removed during the material removal. The position of the finished part in the blank

10.1016/j.procir.2022.04.079

has an impact on the final deformations [6]. Thus, it is possible to optimize the position of the final part in the blank in order to minimize the deformations after machining.

If the process is repeatable, the best position can be found empirically, but it requires a lot of trials. Another solution is to carry out Finite Element Model (FEM) simulations of the relaxation of the residual stresses, but it necessary to know the stress field. For rolled plates, the stress field can be known, because the geometry is simple, and the thermomechanical gradients known [7]. On more complex forming or heat treatment processes, and / or more complicated part geometries, measurements are required. There are two families: destructive and non-destructive. Non-destructive measurement techniques, such as XRD are expensive and difficult to set up and can only analyze the surface of the part. Therefore, it cannot be used on a production line. Techniques like layer removal (destructive technique), involve machining the part by thin layers to reconstruct the residual stress field, as it is done in [8]. This method can be used during machining but requires a lot of machining steps to precisely know the field, which considerably increases the machining time.

However, on forged blanks, the variability of the residual stress field is a major issue and leads to variabilities in the deformations of the machined parts. Plus, it is difficult to use results from other parts as the geometries will differ.

In this paper, a new model of the variability of the stress field induced by forging and heat treatment in large aeronautical structural part is proposed. Firstly, the finite element simulation of each step of the process, from forging to cutting, is introduced. Section 2 also explains how the deformations caused by the residual stress field are computed. Then, a sensibility analysis shows the impact of the key factors on variability. In the last section, a singular value decomposition (SVD) is used to extract a reduced model of the residual stress field variability.

2. Process simulation

2.1. 2D-FEM simulation of the forging steps

The aeronautic case study concerns long cruciform forged part (with a length of several meters, a width of less than a meter in its cross-section and a thickness of few centimeters, cf. Fig 1). One dimension of these cruciform is much larger than the two others. Thus, the proposed approach consists in a coupling of 2D simulations, to show the effect of each process step in the cross-sections of the part, with a beam model to obtain the global deformation of the part, as described by Figure 1. Boundary effects at the extremities of the part are neglected as there are not the areas which contribute the most to the deflection. The global deflection of the part results from cumulative deformations of the cross-sections along the part. Deformations in the middle of the part have a higher impact on the global deflection.

The blank of the cruciform is forged from 7010 aluminum alloy that has been modeled by a Johnson-Cook law with temperature-dependent coefficients. The elastic behavior, the thermal expansion and the specific heat are also temperature dependent.

The part is meshed with 1630 elements of type CPEG4T, which are 4-node generalized plane strain temperature-displacement coupled elements from Abaqus software. The steps are defined in Figure 2.

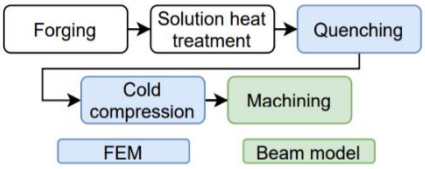

Figure 1 : Manufacturing steps and modelling.

Initialization: stress free, temperature at 20°C.
Step 1, homogenization : homogenization temperature applied on the contour. Coupled Temperature-displacement.
Step 2, quenching: Quenching temperature applied on the contour. Coupled Temperature-displacement.
Step 3, compression: Upper die moves down with compression load. Static.
Step 4, release: Upper die moves up. Static.

Figure 2 : FEM steps.

2.1.1. Quenching

Before quenching the parts undergo a solution heat treatment that is supposed to relieve the residual stresses induced by forging. Hence, at the beginning of the simulation, the part is at 20°C and residual stress free. Then it is heated up to the homogenization temperature. This heat transfer is modeled with a surface film condition and non-temperature dependent thermal exchange coefficient. Quenching is also modeled by imposing a surface film condition to the contour of the part but this time with a temperature-dependent coefficient.

During the heating step and quenching, the out-of-plane d.o.f (degrees of freedom of the 2D FEM) are released to allow out-of-plane expansion, as can be done with generalized strain plane elements.

The gradients of temperature induced during quenching create also gradients of residual stresses in part; with the core being in traction and the skin in compression, as shown in Figure 3.

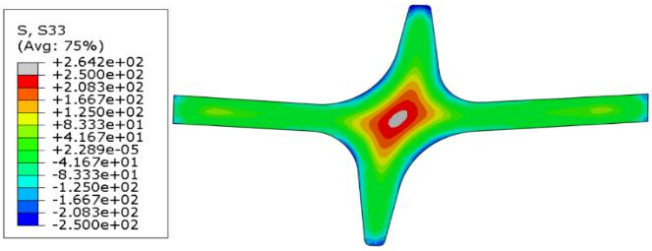

Figure 3 : Out-of-plane stresses after quenching in a cross-section of the part, MPa.

2.1.2. Cold compression

For cold compression, the part mesh remains the same and two compression dies are added in the simulation, meshes with CPEG4T elements too.

These two dies are modeled considering their elastic behavior and thermal expansion. The contact between the dies and the part is modeled with a coulomb law.

Firstly, the dies are heated up and a concentrated load is applied on the second matrix. Then the part is released and gets its final stress field, see Figure 4.

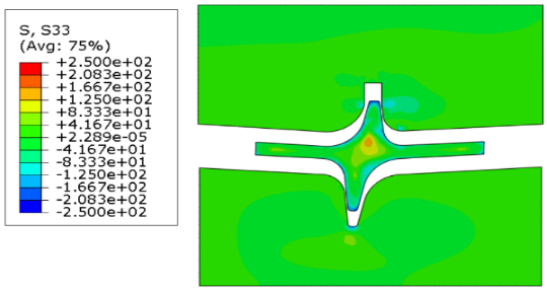

Figure 4 : Out-of-plane stresses after cold compression, MPa.

2.2. Prediction of part distortion

The cruciform is machined from the blank and it deforms in relation to the release of residual stresses. Because of the thickness of the cruciform (~15mm), the machining-induced residual stresses have a limited influence [9] and are here consequently neglected.

The deformations resulting from the residual stress field and their impact on the global deflection of the part is evaluated by computing the bending moment:

$$M_z = \iint_{S_{part}} z.\sigma_{xx}(y,z)ds \quad (1)$$

S_{part} denotes the surface of the section, z the distance to the cross-section's barycenter and σ_{xx} the out-of-plane stresses (along the beam axis X). Only the out-of-plane stress is considered since it has a dominating impact on the deflection. According to the beam theory, the bending moment is linked to the curvature:

$$EI_{Gz}\gamma = M_z \quad (2)$$

With E the Young modulus, I_{Gz} the second moment of area of the cross-section and γ the curvature. Eq 1 and 2 lead to:

$$\gamma = \frac{1}{E.I_{Gz}} \iint_{S_{part}} z.\sigma_{xx}\, ds \quad (3)$$

The cruciform use-case verifies the hypothesis of small displacements (u), thus:

$$\gamma \approx \frac{d^2u}{dx^2} \quad (4)$$

Finally, as the cross-section is discretized, the second derivative of the deformations is obtained from Eq 3 by:

$$\frac{d^2u}{dx^2} = \frac{1}{E.I_{Gz}} \sum_i^N z_i.\sigma_{xx,i}.a_i \quad (5)$$

With $a_i, \sigma_{xx,i}$ respectively the area and the out-of-plane residual stress of the i-th cell. z_i is the vertical distance between the i-th cell and the center of the cross-section. Note that the equations are presented here for the vertical deformations, and similar ones are obtained for the horizontal deformations by replacing z by y.

The out-of-plane residual stresses σ_{xx} are interpolated from the 2D-FEM results, with a linear kernel and the 3 nearest cells. The mesh of the finished part (in black) is placed at its theoretical position, cf. Figure 5; since the aim is here to get a model of the stress field's variability of the forged blank

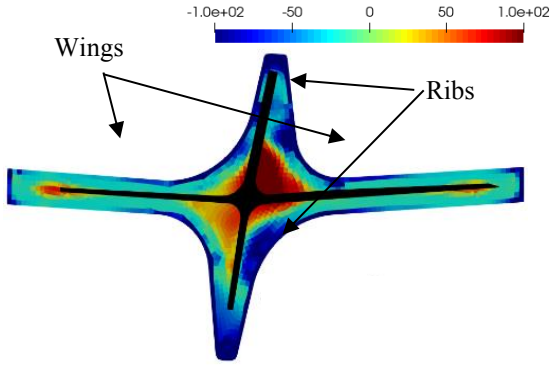

Figure 5 : The final part (in black) in the residual stress field in MPa.

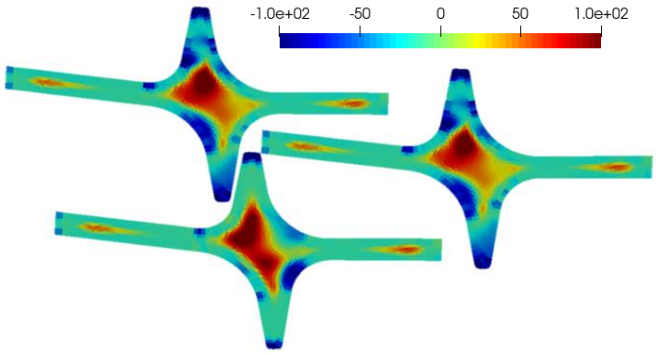

Figure 6: Examples of residual stress fields in MPa (from top to bottom: Nominal, better lubrication, lateral die positioning error).

2.3. Results of sensibility analysis

Simulations have been performed to evaluate the impact of several process parameters on the deflection of the final part, which results from the variability of the residual stress field of the forged blank. Those parameters were chosen based on

empirical knowledge in forging and distortions where computed from eq 5:

- Lubrication
- Longitudinal positioning error of the die
- Transverse positioning error of the die
- Compression load
- Quenching temperature
- Wing thickness
- Difference in wing thickness

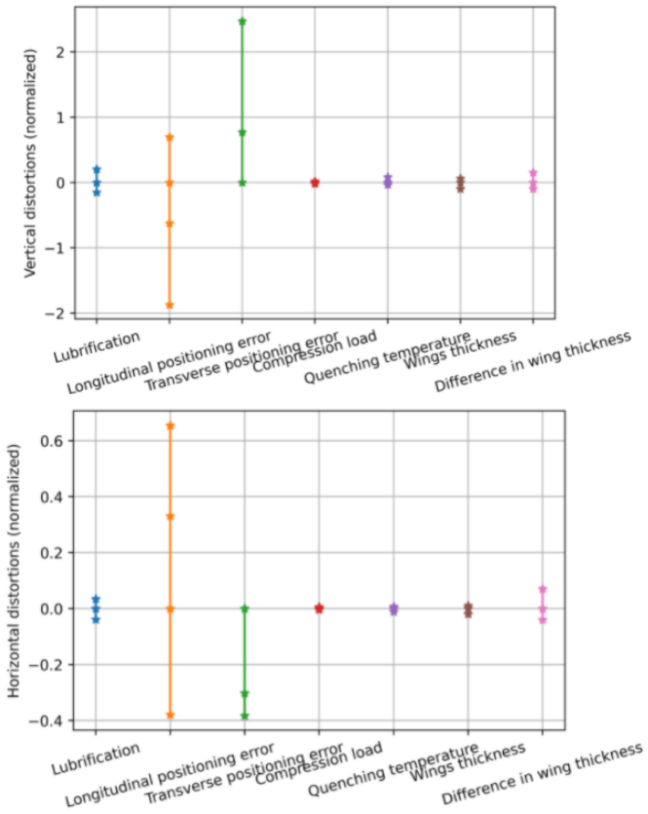

Figure 7 : Comparison of the impact of process parameters on part post-machining deformation, computed with eq 5.

The values tested for each parameter are based on the forger's process variability too, to get realistic simulations of cruciform variability. And 3 examples are shown by Figure 6, the results of the nominal simulation, one with a better lubrication that shows little difference and a last one with an error on the longitudinal positioning of the die.

As shown in Figure 7, the same conclusions can be drawn from the results of horizontal and vertical variability of the deflection. Besides, two parameters have a significant effect on the variability of part distortions: the longitudinal and transverse positioning error of the die. A faulty position of the part in the die, or faulty relative position of the two dies, leads to a variation of the location of the contacts between the dies and the part, especially in the radius. Therefore, it changes the contact area with high compression in the part, which conducts to a different residual stress field. The magnitude of the residual stress field remains the identical, but its shape (locations of extremum values) is impacted. Moreover, as the part distortions are caused by an imbalance in the machined part residual stresses, a significant impact is consequently revealed by the sensibility analysis.

Note that the thickness of the part decreases along its length. Thus, shifting longitudinally a die modifies the compression rate, as well as the residual stress field.

Lubrication has a noticeable impact on the deformations, according to the simulations (represented by the coefficient of friction). A better lubrication leads to an easier material flow in the dies and thus impacts the level of compression during cold compression, especially in the ribs. It also impacts the residual stress field on the surface of the upper rib, as higher friction leads to tensile stresses in this area.

There are almost no variations of the part distortion coming from changes in the compression load or quenching temperature or from the quenching temperature. In fact, the tolerances of the forger process on those parameters are tight (< 5%) which limits in practice their sensitivity. Moreover, regarding compression, the required force to obtain plastic deformation on the part increases significantly once the upper die makes contact with the horizontal wings of the cruciform. Having the compression force that deviates slightly from the nominal value makes then little difference on the final residual stress field in the core and in the ribs. Additionally, the variation induced on the residual stress field is almost symmetrical with respect to the neutral fiber of the machined part and therefore has little impact on the deformations after machining.

When the thickness of the wings varies (but remains identical for both wings), there is no major impact. The outer shape of the part remains unaltered, the contact between the dies and the part leads to the same areas of maximum compression and to the same residual stress field. However, if one wing is slightly thicker than the other one, the compression will be much higher in the first one. It creates an asymmetry in the residual stress field of the wings and consequently impacts the distortions, mainly in the horizontal direction.

The sensibility analysis has enabled the identification of the key factors of the variability of part distortions. They can hence be used to predict part distortion.

Table 1: Range of distortions induced by each parameter.

Parameters	Lubrification	Longitudinal positioning error	Transverse positioning error	Compression load	Quenching temperature	Wings thickness	Difference in wing thickness
Range, normalized by the longitudinal positioning error (%), vertical	13.7	100	96	1.4	4.6	6.2	9.7
Range, normalized by the longitudinal positioning error (%), horizontal	7.1	100	37	0.8	1.7	2.9	10.6

3. Reduced model of the variability of the residual stress field

3.1. Reduced SVD model of residual stress field

In order to predict the part distortion from the key factors previously identified, a model order reduction method is here proposed. The Proper Orthogonal Decomposition (POD) belongs to the family of model order reduction methods and was introduced by [10]. Given a set of data, it provides an orthogonal basis representing them in a lower space, of *r* order, which leads to the following decomposition:

$$u(\boldsymbol{x}) \approx u_r(\boldsymbol{x}) = \sum_{k=1}^{r} \alpha_k(\boldsymbol{x})\boldsymbol{\Phi}_k \quad (6)$$

This method has been successfully applied in fluid dynamics, but applications may be found in other fields such as structural mechanics [11]. In this study, POD is applied to the process of cold compression, based on the simulations developed in section 2.3.

The first step is to take several snapshots [12], that embed the process behavior, thereby each snapshot must be taken in a different location of the parametric space. This phase is important because if a behavior is not included in this training dataset, it will not appear in the reduced model. From the results of the sensibility analysis discussed in 2.3, only two factors are kept to define the parametric space: the longitudinal and transverse positioning errors of the die. Indeed, these two parameters produce most of the variability, see Table 1, and the others have a smaller or no impact on the results. Moreover, it will reduce the number of snapshots needed to build the model. As the POD is a non-intrusive method, the simulation results are directly used (the snapshots). In this study, 25 snapshots were simulated, distributed in the parametric space as shown in Figure 8.

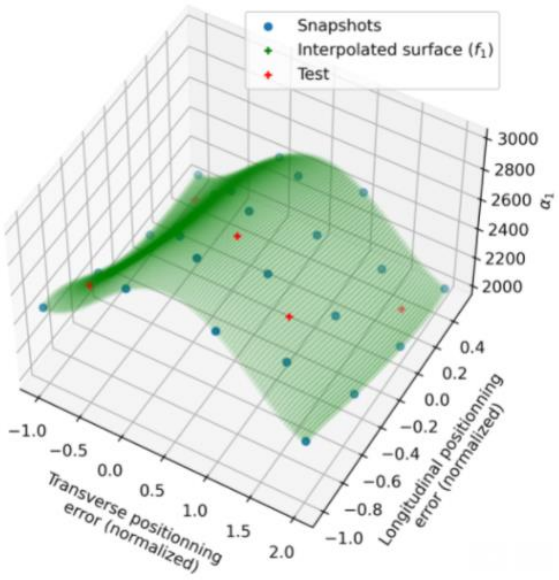

Figure 8 : Link between the process parameters and the SVD reduced model by polynomial regression (here for the first mode coefficient α_1).

The out-of-plane stresses σ_{xx} computed at the center of each cell are extracted and used to define the vector a_i of size $n \times 1$ (n being the number of cells in the i^{th} 2D-FEM simulation). Stacking those vectors gives a matrix A of size $n \times m$, with m the number of simulations.

A Singular Value Decomposition (SVD [13]) is then performed on the matrix A and gives the following decomposition:

$$A = U\Sigma V^T \quad (7)$$

where U is an orthogonal matrix of the left singular vectors of size $n \times n$, and V is an $m \times m$ orthogonal matrix of the right singular vectors. Σ is a $n \times m$ rectangular matrix of the singular values.

The reduced basis is chosen from the r left eigenvectors corresponding to the most energetic eigenvalues, defined by the square of the eigenvalues. The value of r can be chosen from the ratio of the energy as defined in [14]. As the aim of this reduced model is to compute the distortions induced by the stress field variability as explained in section 2.2, a criterion based on the averaged relative error between the deformations caused by the residual stress field from the snapshots and from the reduced model is preferred:

$$e^r = \frac{1}{m}\sum_{i=1}^{m} \frac{\gamma_{r,i} - \gamma_i}{\gamma_i} \quad (8)$$

m denotes the number of snapshots, γ is the curvature due to the bending moment after machining (of which the part distortion derives) and r corresponds to the number of modes Φ used in the reduced basis. If modes associated with singular values of low energy describe a field's feature that does not impact the deformations, it can be neglected. It could due to a low deviation or due to a change in the field in an area where the section of the machined part is not. But the basis should not be reduced too much, as modes of low energy can have minimal influence on the distortion of the machined part but can contribute to the equilibrium of the residual stress field in the blank section.

Table 2 shows the relative error e^r depending on the number r of components considered as computed in Eq 7. The decomposition of the residual stress field in a reduced basis provides a good generalization of the behavior simulated by 2D-FEM. With the first 6 components, an error of 3% is obtained, and of 1% for 12 components. A reduced basis of $r = 6$ modes was thus chosen here and seems promising for the prediction of new stress fields in the following section.

Table 2: Relative error e^r, depending on the number of components in the reduced basis

Number of components (r)	1	5	6	11	19
e^r (%)	41	9.2	3	2.8	1

3.2. Regression model of process parameters

In section 3.1, a matrix decomposition technique has been applied to a set of simulation results, to extract the principal modes of the residual stress field. Henceforth, new residual stress fields can be generated as a linear combination of those modes. Since each mode is independent, any set of α_k coefficients in Eq 6 could be chosen. But doing so would erase the link between the physics of the process (the positioning error of the die during cold compression) and the resulting residual stress field. Moreover, physically impossible stress fields could be potentially generated.

To counter that and keep a model-based approach a polynomial regression is applied, in order to establish a link between the process parameters and the reduced model ones α_k. Since modes are independent, independent regression can be applied to each of them:

$$\alpha_k = f_k(x_1, x_2), \qquad k \in [1, \dots, r]$$

with f_k a polynomial function of the transverse and longitudinal positioning errors (noted respectively x_1 and x_2), of degree 6.

To evaluate the quality of the interpolation, 5 more simulations where performed, inside the parametric space (the red crosses in Figure 8) for testing. The errors of final distortion of the machined forged part was evaluated by Eq 7. A mean relative error of 0.2 % was obtained on the training dataset (initial snapshots) and an error of 0.8% for the test dataset constituted of the 5 new simulation results. These very good results validate the SVD and regressive reduced model of the variability of the residual stress field in machined forged part.

The model can be illustrated by the Figure 9, where one can generate residual stress fields on-line by tuning the longitudinal and transverse positioning error.

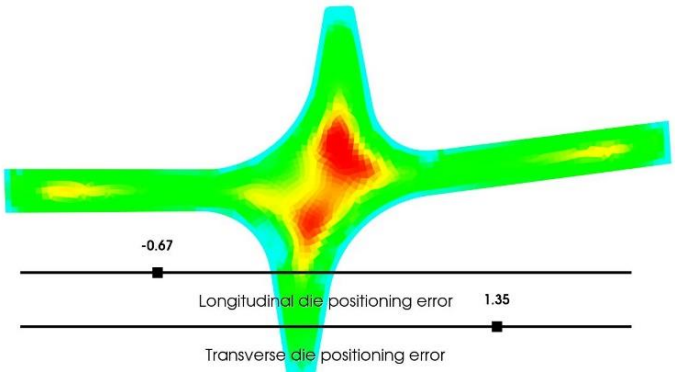

Figure 9 : Resulting reduced model of the residual stress field, controlled by the 2 chosen key process parameters.

4. Conclusion

Variability of the residual stress field of a forged part and its impact on the deformations after machining was investigated through a coupling of 2D-FEM simulation and beam theory, which is particularly suitable for long aeronautic part with complex cross-section geometry.

Sensibility analysis has revealed their impact on the distortion of the machined part considering the variability of the forger's process. It exposed the importance of the positioning of the dies during cold compression.

A model-based approach, with an SVD reduced model controlled by the key process parameters through linear regression was then used to obtain a model of the admissible residual stress fields.

Future work will have to compare those results with measurements on real parts. And use the reduced model to reconstruct residual stress fields from deformations measurements induced by machining.

Acknowledgements

Authors acknowledge the funding of the CIFRE PhD by the French ANRT and Airbus.

References

[1] N. Chobaut, D. Carron, S. Arsène, P. Schloth, et J.-M. Drezet, Quench induced residual stress prediction in heat treatable 7xxx aluminium alloy thick plates using Gleeble interrupted quench tests , *Journal of Materials Processing Technology*, vol. 222, p. 373-380, août 2015, doi: 10.1016/j.jmatprotec.2015.03.029.

[2] B. Denkena, M. Reichstein, et L. de L. Garcia, Milling Induced Residual Stresses in Structural Parts out of Forged Aluminum Alloys , p. 4.

[3] J.-F. Chatelain, J.-F. Lalonde, et A. S. Tahan, Effect of Residual Stresses Embedded within Workpieces on the Distortion of Parts after Machining, vol. 6, nº 1, p. 9, 2012.

[4] Y. Yang, M. Li, et K. R. Li, Comparison and analysis of main effect elements of machining distortion for aluminum alloy and titanium alloy aircraft monolithic component, *Int J Adv Manuf Technol*, vol. 70, nº 9-12, p. 1803-1811, févr. 2014, doi: 10.1007/s00170-013-5431-x.

[5] J. S. Robinson *et al.*, Residual stress in 7449 aluminium alloy forgings, *Materials Science and Engineering: A*, vol. 527, nº 10-11, p. 2603-2612, avr. 2010, doi: 10.1016/j.msea.2009.12.022.

[6] X. Cerutti et K. Mocellin, Influence of the machining sequence on the residual stress redistribution and machining quality: analysis and improvement using numerical simulations, *Int J Adv Manuf Technol*, vol. 83, nº 1-4, p. 489-503, mars 2016, doi: 10.1007/s00170-015-7521-4.

[7] X. Cerutti, S. Arsene, et K. Mocellin, Prediction of machining quality due to the initial residual stress redistribution of aerospace structural parts made of low-density aluminium alloy rolled plates, *Int J Mater Form*, vol. 9, nº 5, p. 677-690, nov. 2016, doi: 10.1007/s12289-015-1254-7.

[8] I. Llanos, M. Aurrekoetxea, A. Agirre, L. N. L. de Lacalle, et O. Zelaieta, On-machine Characterization of Bulk Residual Stresses on Machining Blanks, *Procedia CIRP*, vol. 82, p. 406-410, 2019, doi: 10.1016/j.procir.2019.04.012.

[9] X. Huang, J. Sun, et J. Li, Finite element simulation and experimental investigation on the residual stress-related monolithic component deformation, *Int J Adv Manuf Technol*, vol. 77, nº 5-8, p. 1035-1041, mars 2015, doi: 10.1007/s00170-014-6533-9.

[10] J. Lumley, The structure of inhomogeneous turbulent flows », in *Atmospheric Turbulence and Radio Wave Propagation*, 1967.

[11] V. Buljak, Inverse Analyses with Model Reduction: Proper Orthogonal Decomposition in Structural Mechanics, Springer-Verlag Berlin., vol. 53, 2012.

[12] L. Sirovich, Turbulence and the dynamics of coherent structures. II. Symmetries and transformations, *Quart. Appl. Math.*, vol. 45, nº 3, p. 573-582, 1987, doi: 10.1090/qam/910463.

[13] G. H. Golub, Singular Value Decomposition and Least Squares Sölutions, p. 18.

[14] P. Benner, S. Gugercin, et K. Willcox, A Survey of Projection-Based Model Reduction Methods for Parametric Dynamical Systems, *SIAM Rev.*, vol. 57, nº 4, p. 483-531, janv. 2015, doi: 10.1137/130932715.